Available online at www.sciencedirect.com
SCIENCE DIRECT
Journal of Asian Earth Sciences 27 (2006) 99–107
Journal of Asian Earth Sciences
www.elsevier.com/locate/jaes

Major element geochemistry of glass shards and minerals of the Youngest Toba Tephra in the southwestern South China Sea

Zhifei Liu[a,*], Christophe Colin[b], Alain Trentesaux[c]

[a]Laboratory of Marine Geology, Tongji University, 1239 Siping Road, Shanghai 200092, China
[b]Laboratoire Orsayterre, FRE 2566, BAT. 504, Université de Paris XI, 91 405 Orsay, France
[c]PBDS Laboratory, UMR 8110 CNRS, University of Lille 1, 59 655 Villeneuve d'Ascq, France

Received 16 February 2004; revised 30 December 2004; accepted 16 February 2005

Abstract

An ash layer newly discovered in Core MD01-2393 from the southwestern South China Sea has been studied in order to characterize its major element features. The layer, 4.0-cm thick, light grayish, and silt size, occurs right at the Marine Isotope Stage 4–5 transition, ca. 74 kyr ago. The morphology and geochemistry of glass shards, combined with oxygen isotope and carbonate stratigraphy, confirm the youngest Toba eruption in northern Sumatra as the origin of the ash layer. Major element data on mineral crystals (i.e. biotite, plagioclase, and hornblende) from the ash layer suggest that biotite is phenocrystic while hornblende and some plagioclase are xenocrystic, implying that these xenocrysts were incorporated into the youngest Toba magma before the eruption.

Keywords: Youngest Toba Tephra (YTT); Major elements; Petrogenesis; South China Sea

1. Introduction

The youngest Toba eruption occurred ca. 74 kyr ago and may have been the largest single volcanic eruption of the Quaternary (Rose and Chesner, 1990; Chesner et al., 1991). The impact of this eruption on global climate and human evolution has been widely discussed (Rampino and Self, 1992, 1993; Zielinski et al., 1996; Huang et al., 2001; Oppenheimer, 2002). Dispersed rhyolitic glass and pumice of the Youngest Toba Tephra (YTT) from Toba in northern Sumatra were first found in deep-sea cores in the northeastern Indian Ocean, the Bay of Bengal, the Andaman Sea, and on land in Malaysia (Ninkovich et al., 1978; Ninkovich, 1979). Similar deposits were then reported from the Indian subcontinent (Acharyya and Basu, 1993; Shane et al., 1995), the Central Indian Basin (Pattan et al., 1999), the South China Sea (Bühring et al., 2000; Song et al., 2000), and the Arabian Sea (Pattan et al., 2001; Schulz et al., 2002; Fig. 1). The recovered cores show that dispersal of the YTT extended to 14°S in the southern hemisphere, westwards as far as the longitude 64°E, and northeastwards ~1800 km in the South China Sea, i.e. at least 2% of the Earth surface. Thus, geochemical compositions of glass shards and minerals from deposits of the YTT are usually considered for tephrostratigraphic correlation (Gasparotto et al., 2000; Song et al., 2000). Recent experimental petrology and $^{40}Ar/^{39}Ar$ dating of minerals from the youngest Toba tuff in northern Sumatra suggest that hornblende and some plagioclase are xenocrysts, despite being a major phase in the tuff (Gardner et al., 2002). Hence, potential geochemical variations of hornblende and plagioclase could reflect re-equilibration after their incorporation into the magma. Such xenocrysts have not been previously reported from the YTT marine deposits. This report states, to our knowledge, the first occurrence of xenocrystic hornblende and plagioclase from marine YTT.

Here we present a newly discovered ash layer in Core MD01-2393 in the southwestern South China Sea. The ash layer is identified as the YTT by major element

* Corresponding author. Tel.: +86 21 6598 4877; fax: +86 21 6598 8808.
E-mail address: lzhifei@online.sh.cn (Z. Liu).

1367-9120/$ - see front matter © 2005 Elsevier Ltd. All rights reserved.
doi:10.1016/j.jseaes.2005.02.003

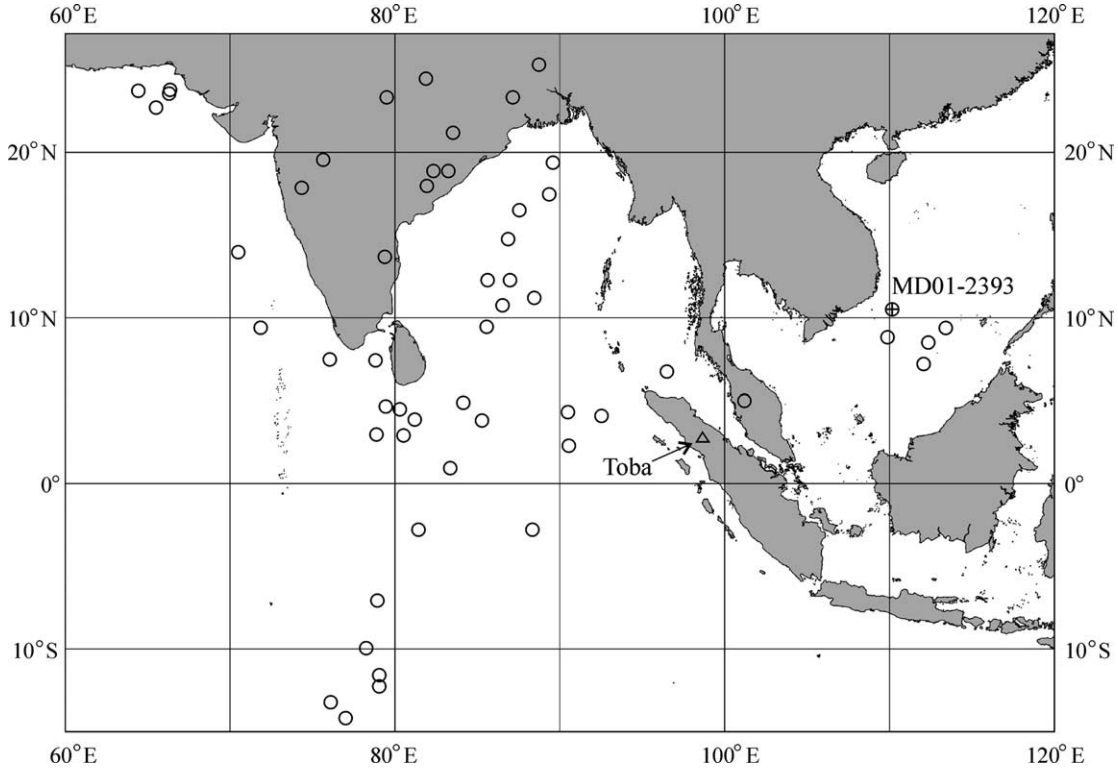

Fig. 1. Distribution of recovered Youngest Toba Tephra (YTT) deposits (open circles) and location of Core MD01-2393 in the southwestern South China Sea (crossed circle). Data from Ninkovich et al. (1978), Rose and Chesner (1987), Acharyya and Basu (1993), Shane et al. (1995), Pattan et al. (1999, 2001), Bühring et al., (2000), Song et al. (2000), Gasparotto et al. (2000) and Schulz et al. (2002).

geochemistry of glass shards combined with oxygen isotope and carbonate stratigraphy. Hornblende and some plagioclase from the layer are considered as xenocrysts and they may improve our knowledge of the petrogenesis of the youngest Toba magma.

2. Analytical techniques

Core MD01-2393 (10°30.15′N, 110°03.68′E, 1230 m water depth) was recovered on the continental slope in the southwestern South China Sea during the IMAGES cruise VII-WEPAMA in 2001 (Fig. 1). Its lithology is homogeneous, dominated by olive gray foraminifera-rich or diatom-bearing nannofossil ooze with terrigenous clay. The 4.0-cm-thick, light grayish ash layer occurs from 1946 to 1950 cm depth, with a sharp lower contact and a slightly undulating upper boundary. There are no obvious disturbances from bottom current and bioturbation.

The ash sample was wet sieved over a 63-μm mesh sieve and dry sieved over a 150-μm mesh sieve. Both grain-size fractions consist almost entirely of glass shards and pumice, with minor individual crystals reaching a maximum size of ~400 μm in diameter (e.g. biotite, plagioclase, and hornblende). The ash particles and minerals were cast in epoxy resin, cut, and polished in order to process further investigation.

Major element contents were analyzed with an electron microprobe Philips XL-30 at the Orsayterre Laboratory, University of Paris XI, using an accelerating voltage of 15 kV and an electron-beam current of 1.9 nA, with the beam defocused to 6 μm width. Measurements were focused on the cores of individual, fresh, glass shards and minerals with well-exposed interiors. We analyzed 27 glass shards, 16 biotite grains, 9 plagioclase grains, and 4 typical hornblende grains. The analytical uncertainty is <5% for major elements.

Oxygen isotopic compositions ($\delta^{18}O$) of Core MD01-2393 have been measured on planktonic foraminifera *Globigerinoides ruber* (white) (250–315 μm) using an Optima VG mass spectrometer at the Laboratoire des Sciences du Climat et de l'Environnement, Gif-sur-Yvette (Liu et al., 2004). The mean external reproducibility of carbonate standards is ±0.07‰ for $\delta^{18}O$. Carbonate contents were determined using the gasometric technique with precision better than ±2% (Liu et al., 2004). Major element and oxygen isotope measurements on samples were conducted on 10–20 cm spaced intervals throughout the core with an average temporal resolution of 0.3 kyr for the interval of 70–78 kyr.

3. Results and discussion

3.1. Age control

The chronology of Core MD01-2393 has been established mainly by correlating planktonic foraminifera *G. ruber* (white) δ^{18}O records with the planktonic foraminifera *Globigerinoides sacculifer* δ^{18}O record of Core MD97-2151 (8°43.73′N, 109°52.17′E, 1550 m water depth), the latter having detailed AMS ^{14}C dates (Lee et al., 1999) for the last 18 kyr. The core was also correlated with the SPECMAP oxygen isotope stratigraphy (Martinson et al., 1987) before 18 kyr (Liu et al., 2004; Fig. 2). The last occurrence (LO) of *G. ruber* (pink) at 127 kyr ago (Lee et al., 1999) occurs at 2855.5 cm in Core MD01-2393. The δ^{18}O values vary between −1.2 and −3.5‰ and indicate interglacial-glacial variations with a mean boundary at −2.5‰ (Fig. 2). Carbonate contents vary between 5 and 22 wt% with higher values reflecting interglacial periods. The parallel carbonate content curve confirms the age scale model (Fig. 2). Here the ash layer forms a well-defined 0% carbonate content at 1946–1947 cm depth, right at the Marine Isotope Stage (MIS) 4–5 transition. Hence, the ash is dated ca. 74 kyr. This age matches previous age estimates for the youngest Toba eruption, deduced from various dating methods such as K/Ar dating (73.5 ± 3 kyr, Ninkovich et al., 1978), ^{40}Ar/^{39}Ar dating (73 ± 4 kyr, Chesner et al., 1991), SPECMAP-based dating of other core records in the South China Sea (ca. 74 kyr, Bühring et al., 2000; Song et al., 2000), and the reviewed average estimate from literature data (74 ± 2 kyr, Oppenheimer, 2002).

3.2. Morphology and geochemistry of glass shards

The optical microscope investigation indicates that glass shards and pumice appear fresh, shining, and colorless with different sizes (mainly 20–500 μm) and shapes with no signs of alteration. Minor biotite grains, with sizes ranging between 100 and 400 μm in diameter, are dark brown in

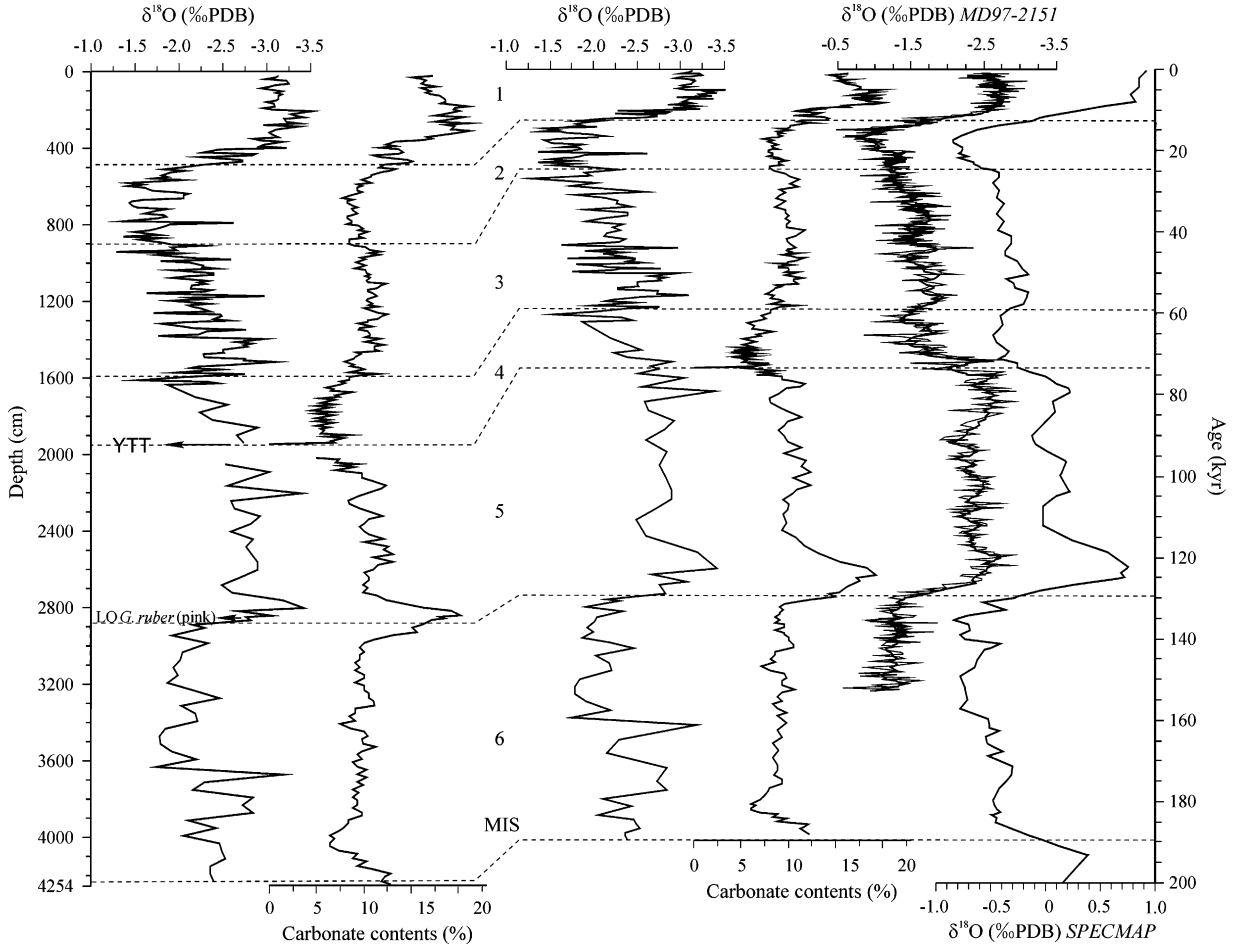

Fig. 2. Planktonic foraminifera *G. ruber* (white) δ^{18}O record and calcium carbonate contents of Core MD01-2393 in both depth (cm) and age (kyr) scales. The YTT layer with 0% carbonate content appears at the Marine Isotope Stage (MIS) 4–5 transition. The last occurrence (LO) of *G. ruber* (pink) is labeled. Planktonic foraminifera *Globigerinoides sacculifer* δ^{18}O record from Core MD97-2151 (Lee et al., 1999) and stacked SPECMAP δ^{18}O (Martinson et al., 1987) are included for their correlation. The data (fine) were smoothed by a five-point moving average (coarse) for the δ^{18}O curve of Core MD97-2151.

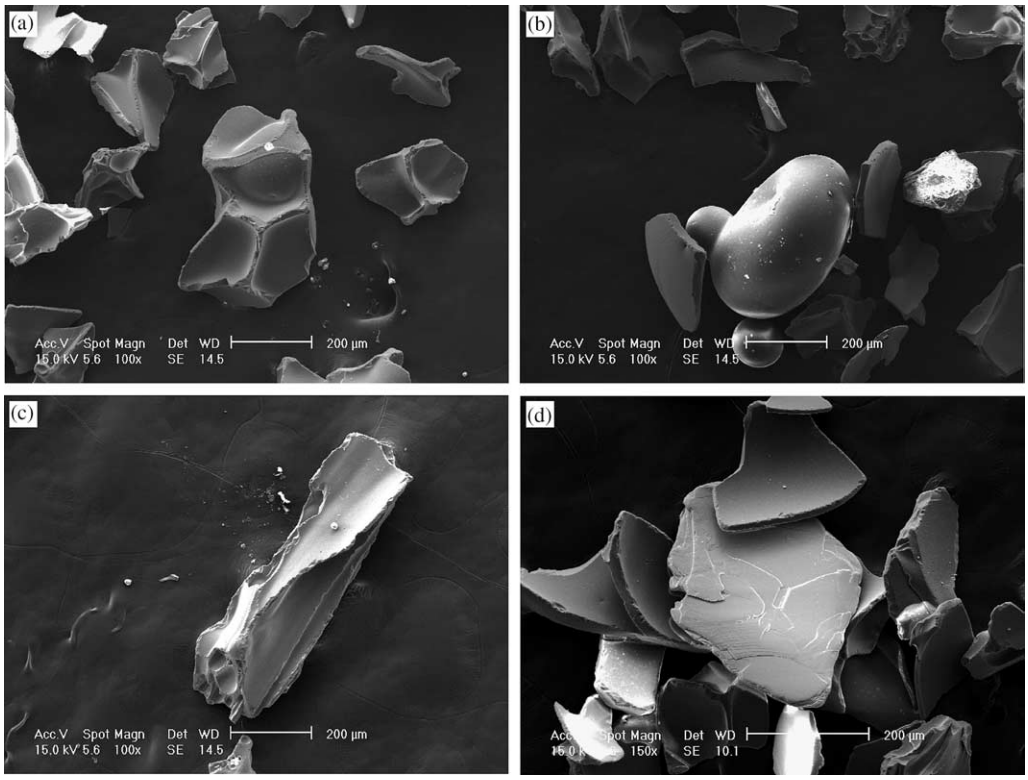

Fig. 3. SEM photomicrographs of Tephra from Core MD01-2393. (a) Bubble-wall shards with smooth and slightly curved surfaces; (b) elongated bubble with two small coalescent ones; (c) pumice shard with elongated vesicles; (d) platy and angular biotite mineral.

color and platy in shape. The very few plagioclase and hornblende grains, with sizes ranging from 50 to 400 μm in diameter, are granular in shape, and gray or dark green in color, respectively.

Additional scanning electron microscopy (SEM) studies on the morphology of the glass shards and minerals show that most of the shards are of the bubble-wall variety with smooth and slightly curved surfaces (Fig. 3a). Shards with junction-type wall fragments suggest remnants of connected bubbles, which are well preserved in our sample (Fig. 3b). Pumice fragments have elongated and parallel vesicles (Fig. 3c). These morphological features suggest that these glass shards are of magmatic origin and very similar to glass shards in other cores from the South China Sea (Bühring et al., 2000; Song et al., 2000), Indian Ocean and the Bay of Bengal (Rose and Chesner, 1987; Gasparotto et al., 2000). In addition, the platy biotite grains are idiomorphic in shape and occur as an associated component with glass shards (Fig. 3d), implying their contemporaneous volcanic origins.

The glass shards have the composition of high-silica rhyolites; their SiO_2 contents are 76.0–77.9 wt%, and they have high Na_2O+K_2O contents of 6.4–7.4 wt% (Table 1). They show very little variation among shard populations. These data show significant differences from the tephra found in the northern South China Sea, with an average SiO_2 content of 56.7 wt% for the latter (Wang et al., 1992). However, their SiO_2, Na_2O, K_2O, FeO* (all Fe as FeO), and Al_2O_3 contents are very similar to those reported for the YTT from other cores in the southern South China Sea (Bühring et al., 2000; Song et al., 2000; Liang et al., 2001), the Indian Ocean and Bay of Bengal (Dehn et al., 1991; Pattan et al., 1999; Gasparotto et al., 2000), Arabian Sea (Schulz et al., 2002), YTT deposits of Toba in northern Sumatra (Chesner, 1998), Malaysia (Ninkovich et al., 1978), and the Indian subcontinent (Shane et al., 1995; Fig. 4; Table 1). The MgO and TiO_2 contents in glass shards of Core MD01-2393 are significantly high compared with those of other marine YTT (Table 1). However, the reason for high MgO and TiO_2 contents in glass shards is unknown and requires further investigation.

In summary, the morphology and geochemistry of glass shards, combined with oxygen isotope and carbonate stratigraphy, suggest the youngest Toba eruption in northern Sumatra as the source of the ash layer in Core MD01-2393 from the southwestern South China Sea.

3.3. Phenocrysts vs. xenocrysts in the YTT

Despite being minor constituents in the ash layer, biotite, plagioclase, and hornblende constitute the major components of phenocrystic minerals of the YTT in Core MD01-2393. Major element analyses of biotite shows very little compositional variation and their average Mg#

Table 1
Major element compositions (on volatile-free basis) of glass shards from Core MD01-2393 and selected literature data

Sample	Location	*n*	SiO_2	Al_2O_3	TiO_2	FeO*	MnO	MgO	CaO	Na_2O	K_2O
MD01-2393[a]	Southwestern South China Sea	27	76.78 (0.48)	13.09 (0.24)	0.23 (0.10)	0.97 (0.12)	0.25 (0.08)	0.87 (0.09)	0.80 (0.11)	2.75 (0.25)	4.26 (0.32)
MD97-2151[b]	Southwestern South China Sea	15	79.38 (0.40)	12.78 (9.21)	0.07 (0.03)	0.89 (0.05)	0.06 (0.05)	0.04 (0.02)	0.75 (0.08)	1.47 (0.11)	4.56 (0.18)
17961–2[c]	Southern South China Sea	20	78.04 (0.24)	12.45 (0.06)	0.05 (0.02)	0.85 (0.05)	0.07 (0.02)	0.06 (0.01)	0.76 (0.03)	2.86 (0.06)	4.86 (0.08)
17962–4[c]	Southern South China Sea	18	78.05 (0.29)	12.52 (0.06)	0.05 (0.01)	0.84 (0.04)	0.07 (0.02)	0.06 (0.01)	0.77 (0.02)	2.78 (0.07)	4.86 (0.05)
ODP1143[d]	Southern South China Sea	14	77.93 (0.44)	12.82 (0.15)	0.05 (0.03)	0.87 (0.03)	0.10 (0.07)	0.02 (0.01)	0.76 (0.07)	2.66 (0.24)	4.79 (0.25)
115KL[e]	Northern Bay of Bengal	22	77.08 (0.25)	12.87 (0.15)		0.84 (0.10)		0.07 (0.06)	0.75 (0.10)	3.13 (0.23)	5.26 (0.14)
ODP758[f]	Southern Bay of Bengal	28	77.54 (0.38)	12.53 (0.19)	0.08 (0.02)	0.83 (0.05)		0.05 (0.02)	0.80 (0.08)	3.02 (0.38)	5.15 (0.14)
NR-54[g]	Central Indian Basin	17	76.80 (0.20)	12.80 (0.12)	0.06 (0.05)	0.96 (0.06)	0.07 (0.04)	0.05 (0.04)	0.80 (0.07)	3.40 (0.09)	5.06 (0.15)
SO130-289KL[h]	Northern Arabian Sea	40	77.74 (0.40)	12.65 (0.18)	0.06 (0.02)	0.91 (0.07)	0.07 (0.03)	0.06 (0.02)	0.72 (0.08)	2.74 (0.50)	5.05 (0.16)
UT1069[i]	Indian subcontinent	9	77.15 (0.17)	12.67 (0.13)	0.06 (0.04)	0.86 (0.05)	0.08 (0.02)	0.06 (0.01)	0.78 (0.08)	3.26 (0.15)	5.08 (0.12)
Kota Tampan[j]	Malaysia		76.09	14.25	0.17	0.84	0.05	0.11	1.05	2.62	4.82
Si Gura Gura[j]	Toba (bulk rock)		71.12	14.12	0.38	2.95	0.06	0.81	1.83	3.45	5.28
63A1-G[k]	Toba		76.83	12.93	0.08	1.21	0.07	0.18	0.94	2.94	4.82
40-A1[k]	Toba (pumice)		71.17	14.27	0.50	3.87	0.09	0.82	2.65	2.91	3.71
30[k]	Toba (welded)		70.42	15.10	0.46	3.32	0.08	0.74	2.80	3.45	3.61

Note: Values represent average and standard deviations (in parentheses) for *n* microprobe analyses; all data were recalculated to 100% for comparative purposes; FeO*, all Fe as FeO; the analytical uncertainty is <5% for major elements of Core MD01-2393.

[a] This study.
[b] Song et al. (2000).
[c] Bühring et al. (2000).
[d] Liang et al. (2001).
[e] Gasparotto et al. (2000).
[f] Dehn et al. (1991).
[g] Pattan et al. (1999).
[h] Schulz et al. (2002).
[i] Shane et al. (1995).
[j] Ninkovich et al. (1978).
[k] Chesner (1998).

(=MgO/(MgO+FeO*)) value of 0.309 is similar to that of the youngest Toba tuff with a value of 0.301 (Chesner, 1998; Table 2). Furthermore, the plot of FeO*/MgO vs. MnO indicates that the biotite from Core MD01-2393 is similar to that of the youngest Toba tuff and significantly different from those of the middle and oldest Toba tuffs (Chesner, 1998; Fig. 5a). Our data are consistent with former studies on the experimental petrogenesis and $^{40}Ar/^{39}Ar$ dating of biotite from the youngest Toba tuff (Gardner et al., 2002), implying that all biotite grains in the YTT of Core MD01-2393 are related to the youngest Toba magma.

Plagioclase compositions from the youngest Toba tuff, including plagioclase grains from the YTT in Core MD01-2393 (Table 2; Fig. 5b), display a large range of SiO_2 contents (58.8–63.1 wt%), overlapping with those of the middle and oldest Toba tuffs (Chesner, 1998; Fig. 5b). We were unable to measure the An composition of plagioclase, but all plagioclase grains contain similar CaO and Na_2O compositions (Table 2), implying that the plagioclase includes isomorphic types between Anorthite and Albite.

Hornblende (according to the Leake (1978) classification) geochemical compositions among the three Toba tuffs in Sumatra are typically different (Fig. 5c; Chesner, 1998). The SEM investigation on typical hornblende grains from the YTT in Core MD01-2393 reveals two domains, i.e. straight cleavage crystals and embayed crystals (Fig. 6). Major element data distinguish the two groups. The straight cleavage crystals (H01, H02, H03, H04, and H05) have relatively high SiO_2 contents of 41.7–43.4 wt% and MnO contents of 0.8–1.1 wt%, while relatively low contents of SiO_2 (37.5–40.2 wt%) and MnO (0.4–0.7 wt%) characterize the embayed crystals (H06, H07, H08, H09, H10, and H11) (Table 2; Fig. 6). The former is close to the geochemical ranges of the youngest and oldest Toba tuffs, while the latter plot within the range of the youngest and middle Toba tuffs (Fig. 5c). We find that TiO_2 and K_2O contents in the embayed crystals exhibit very high values compared to

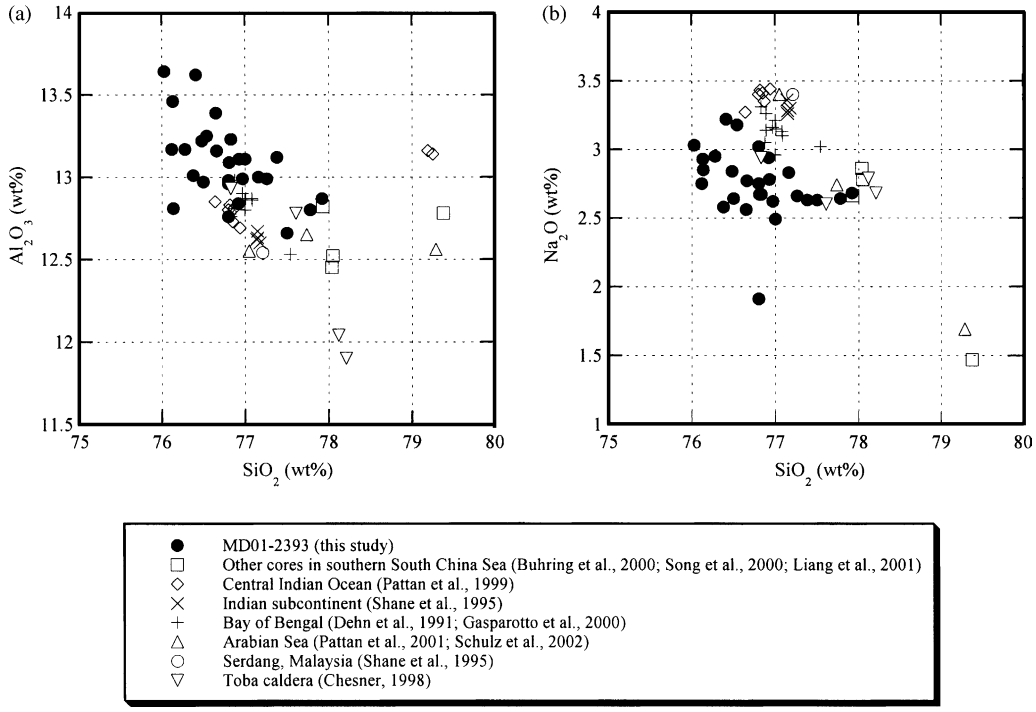

Fig. 4. Geochemical variations of glass shards determined by microprobe analysis. Glass shards from Core MD01-2393 are compared to selected literature data (Table 1). (a) SiO_2 vs. Al_2O_3; (b) SiO_2 vs. Na_2O.

Table 2
Major element compositions of biotite, plagioclase, and hornblende of the YTT from Core MD01-2393 and the Youngest Toba Tuff in Sumatra

Mineral	*n*	SiO_2	Al_2O_3	TiO_2	FeO*	MnO	MgO	CaO	Na_2O	K_2O	Mg#
Biotite, MD01-2393[a]	16	37.58	14.15	4.37	23.01	0.51	10.28	0.20	0.52	9.38	0.309
		(0.55)	(0.26)	(0.24)	(0.46)	(0.13)	(0.36)	(0.15)	(0.14)	(0.18)	
Biotite, Sumatra[b]	3	37.83	14.50	4.25	23.19	0.41	9.99	0.04	0.44	9.35	0.301
		(0.09)	(0.38)	(0.42)	(1.05)	(0.10)	(0.42)	(0.02)	(0.05)	(0.03)	
Plagioclase,	9	58.64	25.31	0.10	0.35	0.02	0.53	6.07	8.18	0.80	0.600
MD01-2393[a]		(0.73)	(0.34)	(0.09)	(0.16)	(0.03)	(0.08)	(0.64)	(0.30)	(0.09)	
Plagioclase, Sumatra[b]	3	60.38	24.63	0.01	0.19	0.02	0.03	6.85	7.14	0.75	0.139
		(1.52)	(0.97)	(0.01)	(0.04)	(0.01)	(0.01)	(1.16)	(0.51)	(0.13)	
Hornblende, MD01-2393[a]											
H01		43.07	8.25	1.41	21.54	1.05	9.76	11.68	2.09	1.15	0.312
H02		42.65	8.41	1.48	21.84	0.89	10.26	10.89	1.88	1.70	0.320
H03		43.39	8.94	1.40	21.05	0.96	10.01	10.94	1.94	1.37	0.322
H04		41.71	8.85	2.07	22.29	0.80	10.29	9.34	1.59	3.06	0.316
H05		43.34	8.65	1.16	20.69	0.90	10.42	11.57	2.16	1.11	0.335
H06		37.46	12.07	4.95	23.70	0.51	10.08	1.23	0.50	9.50	0.298
H07		37.83	11.92	4.38	23.68	0.62	9.55	1.92	0.97	9.13	0.287
H08		39.85	12.42	3.84	21.79	0.44	9.15	3.25	1.43	7.83	0.296
H09		38.59	11.85	4.19	22.56	0.62	10.46	2.83	1.11	7.79	0.317
H10		40.18	10.59	3.13	21.85	0.71	10.31	6.33	1.33	5.57	0.321
H11		39.09	11.46	3.89	22.24	0.48	10.58	3.21	1.32	7.73	0.322
Hornblende, Sumatra[b]	3	45.37	8.67	1.47	20.20	0.75	9.84	10.88	1.95	0.87	0.328
		(0.38)	(0.19)	(0.21)	(1.37)	(0.32)	(1.05)	(0.06)	(0.16)	(0.10)	

Note: Values represent means and standard deviations (in parentheses) for *n* analyses; all data were recalculated to 100% for comparative purposes; FeO*, all Fe as FeO; Mg# = MgO/(MgO + FeO*); the analytical uncertainty is < 5% for major elements of Core MD01-2393; see Fig. 6 for different spots of a typical hornblende from Core MD01-2393.

[a] This study.

[b] Chesner (1998).

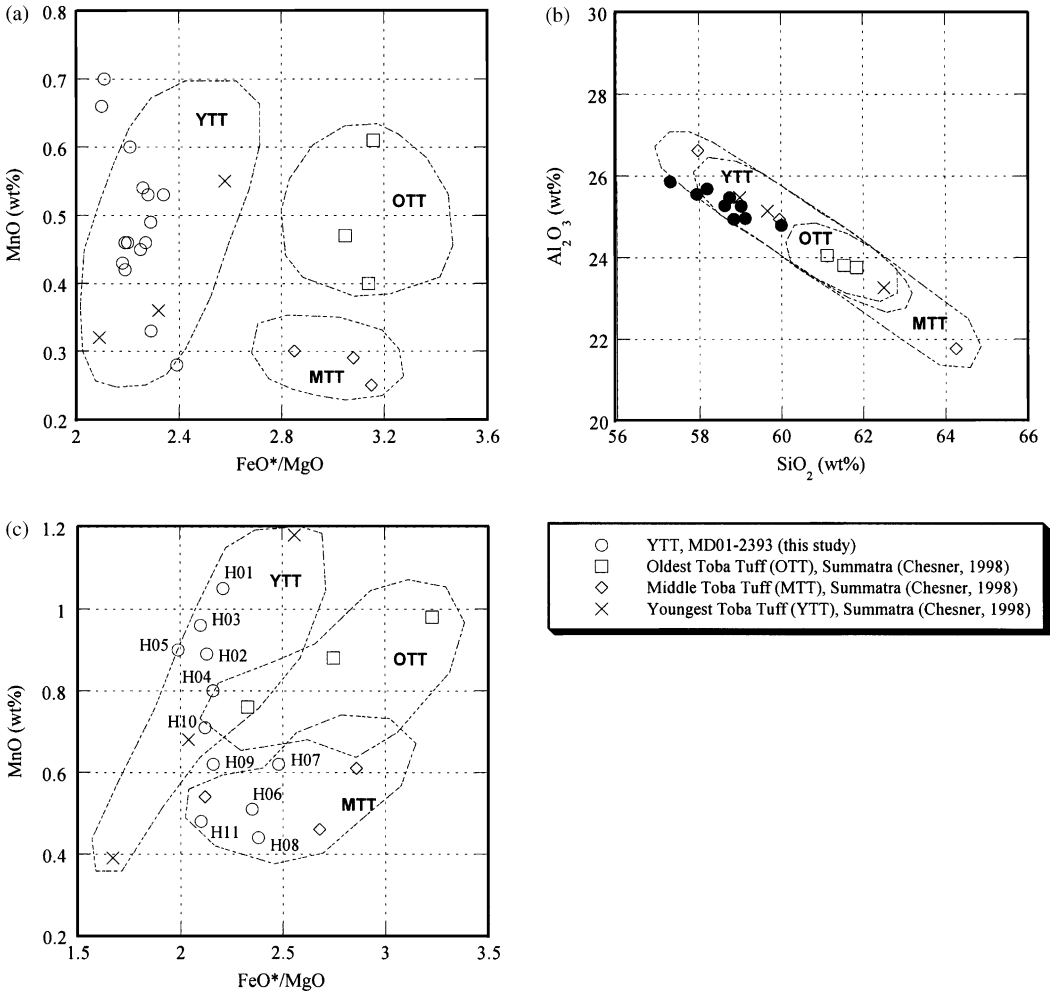

Fig. 5. Mineral compositions from Core MD01-2393 and those of Toba tuffs in Sumatra. (a) FeO*/MgO vs. MnO for biotite; (b) SiO_2 vs. Al_2O_3 for plagioclase; (c) FeO*/MgO vs. MnO for hornblende. FeO*, all Fe as FeO.

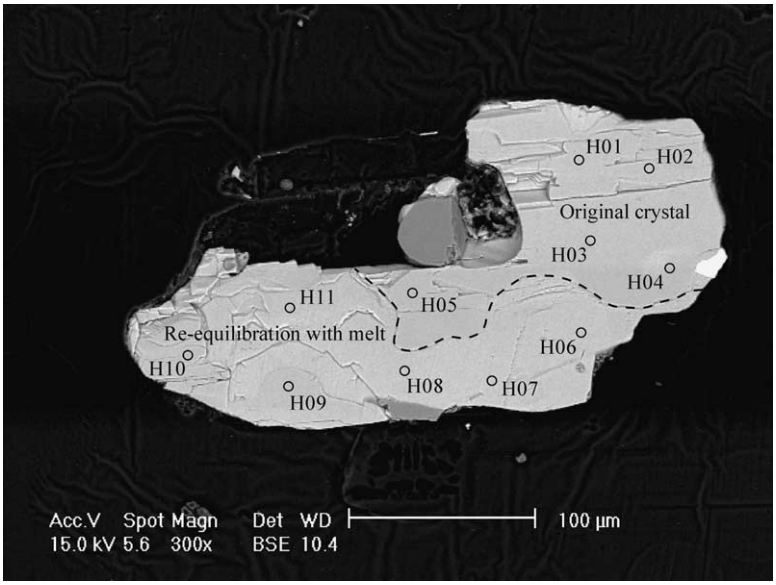

Fig. 6. Photomicrograph of a selected polished hornblende showing various geochemical compositions with different spots (numbered). See Table 2 for major element data.

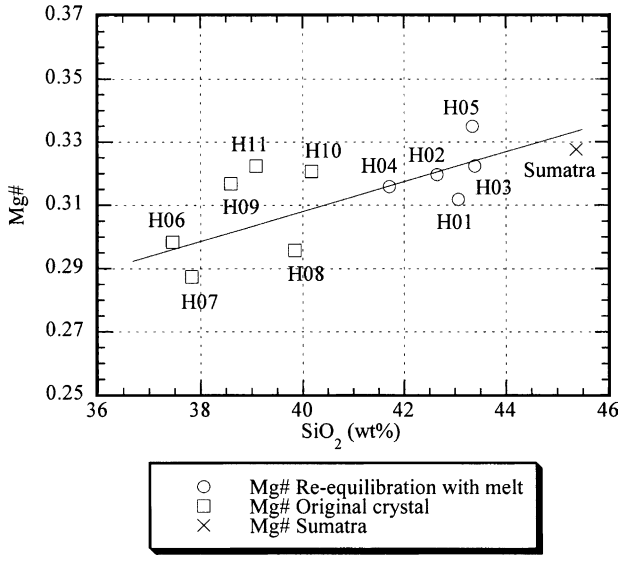

Fig. 7. Compositional characteristics in coordinates of Mg# vs. SiO_2 for hornblende from Core MD01-2393 and Sumatra. Mg#=MgO/(MgO+FeO*); data for hornblende in Sumatra from Chesner (1998); see Table 2 for major element data.

those in hornblende from Sumatra (Table 2). Thus, chemical variations in the embayed crystals and the structure itself may suggest reaction between the crystal and magma.

These geochemical features of plagioclase and hornblende might reveal a complex petrogenetic history for the youngest Toba magma. Experimental petrology suggests that hornblende was not stable in the youngest Toba tuff and $^{40}Ar/^{39}Ar$ dating for all hornblende fractions yield isochron ages between 78 kyr and 1.5 myr (Gardner et al., 2002). Taking into account an isochron age of 452 ± 108 kyr for plagioclase, Gardner et al. (2002) concluded that hornblende and some plagioclase in the youngest Toba tuff are xenocrystic in origin and came from a common source with an age of at least 1.5 myr. Here our new data suggest that the xenocrystic origin of hornblende and plagioclase could result in fewer geochemical differences between the youngest and middle-oldest Toba tuffs for the two xenocrysts, respectively (Fig. 5b and c), because their potential geochemical variations could reflect re-equilibration with the melt.

Our major element geochemical results for hornblende and plagioclase from the YTT in Core MD01-2393 agree with this interpretation. Furthermore, the discrepancy of two optical and geochemical components from one hornblende grain (Fig. 6) suggests that the straight cleavage crystals formed prior to incorporation in the youngest Toba magma. The embayed crystals underwent re-equilibration during the youngest Toba magma formation. The plot of Mg# of hornblende after re-equilibration with melt vs. Mg# of the original hornblende suggests re-equilibration (Fig. 7). High values of TiO_2 and K_2O contents in the embayed crystals may suggest element exchanges with magma during re-equilibration. Our results from YTT in deep-sea cores suggest that biotite is phenocrystic in origin and that hornblende and some plagioclase are xenocrystic in origin, implying that these xenocrysts were incorporated into the youngest Toba magma before the eruption.

4. Conclusions

A newly discovered ash layer in Core MD01-2393 in the southwestern South China Sea is reported. The morphology and geochemistry of glass shards from the core, combined with oxygen isotope and carbonate stratigraphy, confirm the youngest Toba eruption in northern Sumatra as the source of the ash layer. Microprobe and SEM studies on minerals (i.e. biotite, plagioclase, and hornblende) from the YTT suggest that biotite is phenocrystic while hornblende and some plagioclase are xenocrystic, implying that the latter xenocrysts were incorporated into the youngest Toba magma before the eruption.

Acknowledgements

The authors thank the crew and scientists aboard the *RV Marion Dufresne* during the IMAGES VII-WEPAMA cruise in 2001. This research used samples provided by the International Marine Past Global Change Study (IMAGES) program. Maurice Pagel and Giuseppe Siani are warmly thanked for helpful discussions and Rémy Pichon for technical assistance in the laboratory. We especially thank Dr Réjean Hébert and an anonymous reviewer for their constructive reviews that significantly helped to improve this work. This study was supported by the Ministere de la Recherche of France, the National Natural Science Foundation of China (40446003, 40331002, and 40321603), the Shanghai Rising-Star Program (03QE14051), the National Key Basic Research Development Project of China (G2000078500), and the Excellent Young Teachers Program and the Program for New Century Excellent Talents in University of the Ministry of Education of China.

References

Acharyya, S.K., Basu, P.K., 1993. Toba ash on the Indian subcontinent and its implications for correlation of late Pleistocene alluvium. Quaternary Research 40, 10–19.

Bühring, C., Sarnthein, M. Leg 184 Shipboard Scientific Party, 2000. Toba ash layers in the South China Sea: evidence of contrasting wind directions during eruption ca. 74 ka. Geology 28, 275–278.

Chesner, C.A., 1998. Petrogenesis of the Toba Tuffs, Sumatra, Indonesia. Journal of Petrology 39, 397–438.

Chesner, C.A., Rose, W.I., Deino, A., Drake, R., Westgate, J.A., 1991. Eruptive history of Earth's largest Quaternary caldera (Toba, Indonesia) clarified. Geology 19, 200–203.

Dehn, J., Farrell, J.W., Schmincke, H.-U., 1991. Neogene tephrochronology from Site 758 on the northern Ninetyeast Ridge: Indonesian arc volcanism of the past 5 Ma. In: Weissel, J., Peirce, J., Taylor, E. et al. (Eds.), Proceedings of Ocean Drilling Program, Scientific Results 121. Ocean Drilling Program, College Station, TX, pp. 273–295.

Gardner, J.E., Layer, P.W., Rutherford, M.J., 2002. Phenocrysts versus xenocrysts in the youngest Toba Tuff: implications for the petrogenesis of 2800 km^3 of magma. Geology 30, 347–350.

Gasparotto, G., Spadafora, E., Summa, V., Tateo, F., 2000. Contribution of grain size and compositional data from the Bengal Fan sediment to the understanding of Toba volcanic event. Marine Geology 162, 561–572.

Huang, C.-Y., Zhao, M., Wang, C.-C., Wei, G., 2001. Cooling of the South China Sea by the Toba eruption and correlation with other climate proxies ~71,000 years ago. Geophysical Research Letters 28, 3915–3918.

Leake, B.L., 1978. Nomenclature of amphibolites. American Mineralogist 63, 1023–1052.

Lee, M.-Y., Wei, K.-Y., Chen, Y.-G., 1999. High resolution oxygen isotope stratigraphy for the last 150,000 years in the southern South China Sea: Core MD972151. Tao 10, 239–254.

Liang, X., Wei, G., Shao, L., Li, X., Wang, R., 2001. Records of Toba eruptions in the South China Sea: chemical characteristics of the glass shards from ODP 1143A. Science in China (Series D) 44, 871–878.

Liu, Z., Colin, C., Trentesaux, A., Blamart, D., Bassinot, F., Siani, G., Sicre, M.-A., 2004. Erosional history of the eastern Tibetan Plateau since 190 kyr ago: clay mineralogical and geochemical investigations from the southwestern South China Sea. Marine Geology 209, 1–18.

Martinson, D.G., Pisias, N.G., Hays, J.D., Imbrie, J., Moore, T.C., Shackleton, N.J., 1987. Age dating and the orbital theory of the ice ages: development of a high-resolution 0 to 3000,000-year chronostratigraphy. Quaternary Research 27, 1–29.

Ninkovich, D., 1979. Distribution, age and chemical composition of tephra layers in deep-sea sediments off western Indonesia. Journal of Volcanology and Geothermal Research 5, 67–86.

Ninkovich, D., Shackleton, N.J., Abdel-Monem, A.A., Obradovich, J.D., Izett, G., 1978. K–Ar age of the late Pleistocene eruption of Toba, north Sumatra. Nature 276, 574–577.

Oppenheimer, C., 2002. Limited global change due to the largest known Quaternary eruption, Toba ~74 kyr BP. Quaternary Science Reviews 21, 1593–1609.

Pattan, J.N., Shane, P., Banakar, V.K., 1999. New occurrence of Youngest Toba Tuff in abyssal sediments of the Central Indian Basin. Marine Geology 155, 243–248.

Pattan, J.N., Shane, P., Pearce, N.J.G., Banakar, V.K., Parthiban, G., 2001. An occurrence of ~74 ka Youngest Toba Tephra from the Western Continental Margin of India. Current Science 80, 1322–1326.

Rampino, M.R., Self, S., 1992. Volcanic winter and accelerated glaciation following the Toba super-eruption. Nature 359, 50–52.

Rampino, M.R., Self, S., 1993. Bottleneck in human evolution and the Toba eruption. Science 262, 1955.

Rose, W.I., Chesner, C.A., 1987. Dispersal of ash in the great Toba eruption, 75 ka. Geology 15, 913–917.

Rose, W.I., Chesner, C.A., 1990. Worldwide dispersal of ash and gases from earth's largest known eruption: Toba, Sumatra, 75 ka. Palaeogeography, Palaeoclimatology, Palaeoecology 89, 269–275.

Schulz, H., Emeis, K.-C., Erlenkeuser, H., Rad, U.V., Rolf, C., 2002. The Toba volcanic event and interstadial/stadial climates at the marine isotopic stage 5 to 4 transition in the northern Indian Ocean. Quaternary Research 57, 22–31.

Shane, P., Westgate, J., Williams, M., Korisettar, R., 1995. New geochemical evidence for the Youngest Toba Tuff in India. Quaternary Research 44, 200–204.

Song, S.-R., Chen, C.-H., Lee, M.-Y., Yang, T.F., Iizuka, Y., Wei, K.-Y., 2000. Newly discovered eastern dispersal of the youngest Toba Tuff. Marine Geology 167, 303–312.

Wang, H., Zhou, F., Jian, Z., 1992. Volcanic clasts in the periplatform carbonate ooze near the Zhongsha Islands and their bearing on the paleoenvironment (in Chinese with English abstract). In: Ye, Z., Wang, P. (Eds.), Contributions to Late Quaternary Paleoceanography of the South China Sea. Qingdao Ocean University Press, Qingdao, pp. 42–55.

Zielinski, G.A., Mayewski, P.A., Meeker, L.D., Whitlow, S., Twikler, M.S., 1996. Potential atmospheric impact of the Toba mega-eruption ~71,000 years ago. Geophysical Research Letters 23, 837–840.